Article

Copper(I) 1,2,4-Triazolates and Related Complexes: Studies of the Solvothermal Ligand Reactions, Network Topologies, and Photoluminescence Properties

Jie-Peng Zhang, Yan-Yong Lin, Xiao-Chun Huang, and Xiao-Ming Chen

J. Am. Chem. Soc., **2005**, 127 (15), 5495-5506• DOI: 10.1021/ja042222t • Publication Date (Web): 25 March 2005

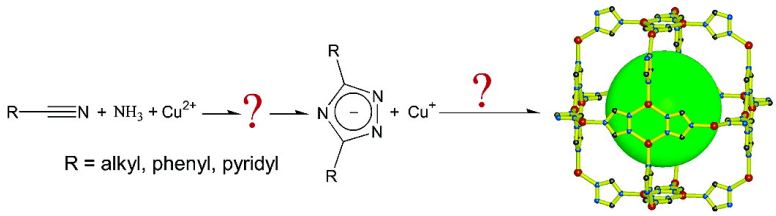

More About This Article

Additional resources and features associated with this article are available within the HTML version:

- Supporting Information
- Links to the 28 articles that cite this article, as of the time of this article download
- Access to high resolution figures
- Links to articles and content related to this article
- Copyright permission to reproduce figures and/or text from this article

View the Full Text HTML

J|A|C|S
ARTICLES
Published on Web 03/25/2005

Copper(I) 1,2,4-Triazolates and Related Complexes: Studies of the Solvothermal Ligand Reactions, Network Topologies, and Photoluminescence Properties

Jie-Peng Zhang, Yan-Yong Lin, Xiao-Chun Huang, and Xiao-Ming Chen*

Contribution from the School of Chemistry and Chemical Engineering, Sun Yat-Sen University, Guangzhou 510275, China

Received December 26, 2004; E-mail: cescxm@zsu.edu.cn

Abstract: One-pot solvothermal treatments of organonitriles, ammonia, and Cu^{II} salts yielded Cu^{I} and 3,5-disubstituted 1,2,4-triazolates. The organic triazolate components were derived from copper-mediated oxidative cycloaddition of nitriles and ammonia, in which a key intermediate 1,3,5-triazapentadienate was isolated as $[Cu^{II}(4\text{-pytap})_2]$ (4-Hpytap = 2,4-di(4-pyridyl)-1,3,5-triazapentadiene) via controlled solvothermal conditions. This intermediate could also be synthesized by Ni^{II}-mediated reactions; however, the final triazoles were obtained only when Cu^{II} was employed. Therefore, the reaction mechanism of these reactions was elucidated as follows: nitrile was first attacked by ammonia to form the amidine, which further reacted with another nitrile or self-condensed to yield 1,3,5-triazapentadiene, which was coordinated to two Cu^{II} ions in its deprotonated form. A two-electron oxidation of the 1,3,5-triazapentadienate mediated by two Cu^{II} ions gave one triazolate and Cu^{I} cations. Other in situ ligand reactions, such as C−C bond cleavage and hydrolysis, were also found for the nitriles under these solvothermal conditions. Another remarkable feature of these crystalline Cu^{I} triazolates is their simple, typical 3- or 4-connected network topologies. The self-assembly of these nets is presumably controlled by steric hindrance, which is subsequently applied to the rational design of the close-packed 2D networks $[Cu^{I}(tz)]_\infty$ and $[Ag^{I}(tz)]_\infty$ (Htz = 1,2,4-triazole), as well as the porous 3D network $[Cu^{I}(etz)]_\infty$ (Hetz = 3,5-diethyl-1,2,4-triazole). The interesting photoluminescence properties of these coinage d^{10} metal complexes were also investigated.

Introduction

The design and synthesis of coordination polymers are of great interest for their intriguing architectures and potential applications. Network topology is a very powerful tool in analyzing complicated coordination polymers.[1,2] Although some target networks could be successfully constructed by the combined use of metal ions and suitable ligands or robust secondary building units (SBUs) with pre-organized geometries and connectivities,[3,4] true crystal engineering of coordination polymers with desirable properties still remains a distant prospect.[3] One of the major problems may be attributed to the complexity of one-pot assembly in a multicomponent system, such as the flexible coordination modes of the commonly used ligands. Polypyridines can afford more predictable coordination modes than carboxylic acids and (pseudo)halides and have been used to reasonably design and assembe finite architectures (thermodynamic requirement favored) with coordination strict metal cations.[5] However, pyridine-like ligands also have limitations for the charge-balance requirement; neutral frameworks cannot be synthesized using only neutral pyridine-like ligands and metal ions. From the crystal engineering and crystal structure prediction point of view, the most viable targets should be the simple topologies by use of simple ligands (predictable coordination modes) and fewer components.[4] Compared to the two-component metal-carboxylate and three-component metal-pyridine-anion systems, binary metal azolates appear to be better candidates for the predictable assembly of coordination polymers. Polyazaheteroaromatic compounds such as pyrazole, imidazole, triazole, tetrazole, as well as their derivatives are well-known for the importance in industry and are widely used as ligands in the neutral and anionic forms.[6−12] The simple binary metal azolates were relatively less-studied due to the

(1) Wells, A. F. *Three-Dimensional Nets and Polyhedra*; Wiley: New York, 1977.
(2) (a) Batten, S. R.; Robson, R. *Angew. Chem., Int. Ed.* **1998**, *37*, 1461−1494. (b) Carlucci, L.; Ciani, G.; Proserpio, D. M. *Coord. Chem. Rev.* **2003**, *246*, 247−289.
(3) Robson, R. *J. Chem. Soc., Dalton Trans*. **2000**, 3735−3744.
(4) (a) O'Keeffe, M.; Eddaoudi, M.; Li, H.-L.; Reineke, T.; Yaghi, O. M. *J. Solid State Chem*. **2000**, *152*, 3−20. (b) Friedrichs, O. D.; O'Keeffe, M.; Yaghi, O. M. *Acta Crystallogr., Sect. A* **2003**, *59*, 22−27. (c) Yaghi, O. M.; O'Keeffe, M.; Ockwig, N. W.; Chae, H. K.; Eddaoudi, M.; Kim, J. *Nature* **2003**, *423*, 705−714.
(5) Leininger, S.; Olenyuk, B.; Stang, P. J. *Chem. Rev*. **2000**, *100*, 853−907.
(6) Potts, K. T. *Chem. Rev.* **1961**, *61*, 87−127.
(7) Haasnoot, J. G. *Coord. Chem. Rev.* **2000**, *200−202*, 131−185.
(8) Masciocchi, N.; Moret, M.; Cairati, P.; Sironi, A.; Ardizzoia, G. A.; La Monica, G. *J. Am. Chem. Soc*. **1994**, *116*, 7668−7676.
(9) (a) Masciocchi, N.; Moret, M.; Cairati, P.; Sironi, A.; Ardizzoia, G. A.; La Monica, G. *J. Chem. Soc., Dalton Trans*. **1995**, 1671−1675. (b) Masciocchi, N.; Castelli, F.; Forster, P. M.; Tafoya, M. M.; Cheetham, A. K. *Inorg. Chem*. **2003**, 6147−6152. (c) Masciocchi, N.; Ardizzoia, G. A.; Brenna, S.; Castelli, F.; Galli, S.; Maspero, A.; Sironi, A. *Chem. Commun*. **2003**, 2018−2019.
(10) (a) Huang, X.-C.; Zhang, J.-P.; Lin, Y.-Y.; Yu, X.-L.; Chen, X.-M. *Chem. Commun*. **2004**, 1100−1101. (b) Huang, X.-C.; Zhang, J.-P.; Chen, X.-M. *J. Am. Chem. Soc*. **2004**, *126*, 13218−13219.
(11) Tian, Y.-Q.; Cai, C.-X.; Ren, X.-M.; Duan, C.-Y.; Xu, Y.; Gao, S.; You, X.-Z. *Chem.−Eur. J*. **2003**, *9*, 5673−5685.

limited solubility of these compounds except the pyrazolates.[8] Ab initio X-ray powder diffraction was hence used to reveal the crystal structures of Ag^{I}, Cd^{II}, Hg^{II}, and Cu^{II} imidazolates.[9] Recently, it has been found that solvothermal (including hydrothermal) conditions are feasible for the synthesis of X-ray quality single crystals of Cu^{I}, $Cu^{I,II}$,[10] Ni^{II},[9b] and Co^{II} imidazolates in the binary form or with different neutral guests.[11]

Solvothermal conditions are widely used in the synthesis of inorganic materials and coordination polymers, and occasionally, some unexpected and important ligand reactions occurred in these processes.[12−17] Furthermore, supramolecular architectures with in situ generated ligands, especially those inaccessible by direct preparation, are of great interest as they can help stabilize unstable species,[18] discovering new organic reactions[12−17,19−27] and understanding the reaction mechanisms.[13,24−28] We may also use some new reactions as facile synthetic methods of corresponding ligands and/or further extend them to rational crystal engineering.[29−31] Although many examples have been obtained under conventional conditions,[19−27] the relatively high temperature and pressure, as well as the presence of transition metal ions in solvothermal conditions, may facilitate some reactions unreachable by conventional methods. On the other hand, the complicated courses involved in the organic reactions or supramolecular assemblies could hardly be "seen" in the one-pot, black-box-like solvothermal reactions, and no in depth investigation on the reaction mechanism of multistep organic ligand reaction under solvothermal conditions was described thus far.

In a recent communication, we reported two Cu^{I} 1,2,4-triazolates coordination polymers with interesting network topologies prepared containing in situ generated ligands under solvothermal conditions. We then proposed a network construction rule based on steric repulsion between rigid square-planar nodes for the important topologies and speculated that the triazolato rings were formed by the oxidative cycloaddition of nitriles and ammonia in 2:1 stoichiometry.[12] Although this reaction has been extended to the rational design of very interesting supramolecular isomers,[31] when the N−N bond forms and the location of the ammonia nitrogen atom are still unclear. Since ammonia may also be produced by hydrolyses of the nitriles, all of the three nitrogen atoms might come exclusively from the nitriles.

As an extension of our previous work, we report herewith our systematic investigation on the ligand formation mechanism and network construction, as well as the interesting photoluminescence properties of these compounds.

Experimental Section

Materials and Physical Measurements. Commercially available reagents were used as received without further purification. Infrared spectra were obtained from KBr pellets on a Bruker EQUINOX 55 Fourier transformation infrared spectrometer in the 400−4000 cm^{-1} region. Elemental analyses (C, H, N) were performed on a Perkin-Elmer 240 elemental analyzer. ESI-MS spectra were performed on a Thermo Finigan LCQ DECA XP ion trap mass spectrometer. Steady-state photoluminescence spectra and lifetime measurements were performed on an Edinburgh FLS920 spectrometer equipped with a continuous Xe900 Xenon lamp, a μF900 microsecond flash lamp, and an nF900 nanosecond flash lamp. In all cases, single crystalline samples were used for the photoluminescence measurements. The μF900 microsecond flash lamp was used in measurements for samples with lifetimes longer than 5 μs, otherwise the nF900 nanosecond flash lamp was used. Lifetime data were fitted with single or double exponential decay functions (for details see Supporting Information).

Typical Synthetic Procedures. [Cu(mtz)]$_\infty$ (**1**; Hmtz = 3,5-Dimethyl-1,2,4-triazole). A mixture of $Cu(OH)_2$ (0.196 g, 2.0 mmol) or $Cu_2(OH)_2CO_3$ (0.221 g, 2.0 mmol), aqueous ammonia (25%, 2.0 mL), and acetonitrile (5.0 mL) was sealed in a 15-mL Teflon-lined reactor and heated in an oven at 120 °C for 60 hrs and slowly cooled to room temperature. The resulting mixture was washed with water, and pale yellow blocklike crystals were collected and dried in air (yield 20−25% based on Cu). Anal. Calcd (%) for $C_4H_6CuN_3$: C, 30.09; H, 3.79; N, 26.32. Found: C, 30.05; H, 3.83; N, 26.28. IR: 3425m, 2960s, 2919s, 1487vs, 1415vs, 1366vs, 1332vs, 1090m, 1040m, 974m, 768m, 693m, 624m cm^{-1}.

{[Cu(etz)]·H$_2$O}$_\infty$ (**2**; Hetz = 3,5-Diethyl-1,2,4-triazole). The reaction was carried out in a method similar to that for **1**, using propionitrile instead of acetonitrile. After being cooled to room temperature, the reactor was left to stand for 1 day. The reactor should remain well-sealed in this period, since crystallization of **2** seemed slow and the Cu^{I} may be oxidized upon exposure to the atmosphere before the crystallization. The resulting mixture was washed with ethanol, and pale yellow blocklike crystals were collected and dried in air (yield 10−15% based on Cu). Anal. Calcd (%) for $C_6H_{12}CuN_3O$: C, 35.03; H, 5.88; N, 20.43. Found: C, 35.25; H, 5.73; N, 20.58. IR: 3425m, 2968vs, 2929vs, 2871s, 1630w, 1500vs, 1473vs, 1354s, 1308s, 1246m, 1068s, 1046s, 975w cm^{-1}.

[Cu(ptz)]$_\infty$ (**3**; Hptz = 3,5-Dipropyl-1,2,4-triazole). The reaction was carried out in a method similar to that for **1**, using butyronitirle instead of acetonitrile. The resulting mixture was washed with ethanol, and pale yellow blocklike crystals were collected and dried in air (yield 10−15% based on Cu). Anal. Calcd (%) for $C_8H_{14}CuN_3$: C, 44.53; H,

(12) Zhang, J.-P.; Zheng, S.-L.; Huang, X.-C.; Chen, X.-M. *Angew. Chem., Int. Ed.* **2004**, *43*, 206−209.
(13) Huang, X.-C.; Zheng, S.-L.; Zhang, J.-P.; Chen, X.-M. *Eur. J. Inorg. Chem.* **2004**, 1024−1029.
(14) (a) Zhang, X.-M.; Tong, M.-L.; Chen, X.-M. *Angew. Chem., Int. Ed.* **2002**, *41*, 1029−1031. (b) Zhang, X.-M.; Tong, M.-L.; Gong, M.-L.; Lee, H.-K.; Luo, L.; Li, K.-F.; Tong, Y.-X.; Chen, X.-M. *Chem.−Eur. J.* **2002**, *8*, 3187−3194.
(15) Zhang, X.-M.; Hou, J.-J.; Wu, H.-S. *J. Chem. Soc., Dalton Trans.* **2004**, 3437−3439.
(16) (a) Evans, O. R.; Lin, W.-B. *Acc. Chem. Res.* **2002**, *35*, 511−522. (b) Lu, J. Y. *Coord. Chem. Rev.* **2003**, *246*, 327−347.
(17) (a) Liu, C.-M.; Gao, S.; Kou, H.-Z. *Chem. Commun.* **2001**, 1670−1671. (b) Wang, R.-H.; Hong, M.-C.; Luo, J.-H.; Cao, R.; Weng, J.-B. *Chem. Commun.* **2003**, 1018−1019.
(18) (a) Lam, C.-K.; Mak, T. C. W. *Angew. Chem., Int. Ed.* **2001**, *40*, 3453−3455. (b) Lam, C.-K.; Chan, T. L.; Mak, T. C. W. *CrystEngComm.* **2004**, *6*, 290−292.
(19) Kryatov, S. V.; Nazarenko, A. Y.; Smith, M. B.; Rybak-Akimova, E. V. *Chem. Commun.* **2001**, 1174−1175.
(20) Kopylovich, M. N.; Pombeiro, A. J. L.; Fischer, A.; Kloo, L.; Kukushkin, V. Y. *Inorg. Chem.* **2003**, *42*, 7239−7248.
(21) Kajiwara, T.; Kamiyama, A.; Ito, T. *Chem. Commun.* **2001**, 1174−1175.
(22) Tong, M.-L.; Wu, Y.-M.; Tong, Y.-X.; Chen, X.-M.; Chang, H.-C.; Kitagawa, S. *Eur. J. Inorg. Chem.* **2003**, 2385−2388.
(23) Drew, M. G. B.; Yates, P. C.; Trocha-Grimshaw, J.; McKillop, K. P.; Nelson, S. M. *Chem. Commun.* **1985**, 262−263.
(24) Lu, T.-B.; Zhuang, X.-M.; Li, Y.-W.; Chen, S. *J. Am. Chem. Soc.* **2004**, 262−263.
(25) Constable, E. C. *Metals and Ligand Reactivity*; VCH: Weinheim, Germany, 1996.
(26) Michelin, R. A.; Mozzon, M.; Bertani, R. *Coord. Chem. Rev.* **1996**, *147*, 299−338.
(27) KukuShkin, V. Y.; Pombeiro, A. J. L. *Chem. Rev.* **2002**, *102*, 1771−1802.
(28) Xiong, R.-G.; Xue, X.; Zhao, H.; You, X.-Z.; Abrahams, B. F.; Xue, Z.-L. *Angew. Chem., Int. Ed.* **2002**, *41*, 3800−3803.
(29) (a) Zheng, S.-L.; Zhang, J.-P.; Wong, W.-T.; Chen, X.-M. *J. Am. Chem. Soc.* **2003**, *125*, 6882−6884. (b) Zheng, S.-L.; Zhang, J.-P.; Chen, X.-M.; Huang, Z.-L.; Lin, Z.-Y.; Wong, W.-T. *Chem.−Eur. J.* **2003**, *9*, 3888−3896.
(30) (a) Zhang, J.-P.; Wang, Y.-B.; Huang, X.-C.; Lin, Y.-Y.; Chen, X.-M. *Chem.−Eur. J.* **2005**, *11*, 552−561. (b) Zhang, J.-P.; Huang, X.-C.; Lin, Y.-Y., Chen, X.-M. *Inorg. Chem.*, in press.
(31) Zhang, J.-P.; Lin, Y.-Y.; Huang, X.-C.; Chen, X.-M. *Chem. Commun.* **2005**, 1258−1260.

6.54; N, 19.48. Found: C, 44.60; H, 6.50; N, 19.39. IR: 3440m, 2959vs, 2930vs, 2873vs, 1496vs, 1461vs, 1354vs, 1274s, 1224s, 1079s, 901m, 825m, 746m cm^{-1}.

$[Cu_5CN(btz)_4]_\infty$ (**4**; Hbtz = 3,5-Dibutyl-1,2,4-triazole). A mixture of $Cu(OH)_2$ (0.196 g, 2.0 mmol), aqueous ammonia (25%, 1.0 mL), valeronitrile (1.0 mL), and THF (5.0 mL) was sealed in a 15-mL Teflon-lined reactor and heated in an oven at 120 °C for 60 hrs and slowly cooled to room temperature. The resulting mixture was washed with ethanol, and colorless blocklike crystals were collected and dried in air (yield ca. 5% based on Cu). Anal. Calcd (%) for $C_{41}H_{72}Cu_5N_{13}$: C, 46.25; H, 6.82; N, 17.10. Found: C, 46.12; H, 6.68; N, 16.98. IR: 3431w, 2956vs, 2927vs, 2869s, 2111m, 1505vs, 1457vs, 0.1072s, 1076m cm^{-1}.

$[Cu_6(phtz)_6]_\infty$ (**5**; Hphtz = 3,5-Diphenyl-1,2,4-triazole). The reaction was carried out in a method similar to that for **1**, using benzonitrile instead of acetonitrile. The resulting mixture was washed with ethanol, and the yellow crystals were collected and dried in air (yield 5−10% based on Cu). Anal. Calcd (%) for $C_{84}H_{60}Cu_6N_{18}$: C, 59.25; H, 3.55; N, 14.81. Found: C, 59.40; H, 3.50; N, 14.69. IR: 3017m, 2918m, 2862m, 1613m, 1436vs, 1328m, 1182m, 1109m, 1015m, 822vs, 954s cm^{-1}.

$[Cu^I_2Cu^{II}_2(2\text{-pytz})_4(2\text{-pa})_2]\cdot 2H_2O$ (**6**; 2-Hpytz = 3,5-Di(2-pyridyl)-1,2,4-triazole, 2-Hpa = Pyridine-2-carboxylic acid). A mixture of $Cu(OH)_2$ (0.196 g, 2.0 mmol), aqueous ammonia (25%, 1.0 mL), and 2-cyanopyridine (1.04 g, 10 mmol) was sealed in a 15-mL Teflon-lined reactor and heated in an oven at 90 °C for 60 hrs and slowly cooled to room temperature. The resulting mixture was washed with water and dried in air, and brown blocklike crystals were manually separated from the red ones[31] (yield ca. 2% based on Cu). Anal. Calcd (%) for $C_{60}H_{44}Cu_4N_{22}O_6$: C, 50.63; H, 3.12; N, 21.65. Found: C, 50.71; H, 2.98; N, 21.81. IR: 3435m, 3018m, 1680s, 1617s, 1494m, 1422s, 1350s, 1198m, 1051m, 932m, 776m, 684m cm^{-1}.

$\{[Cu_5(3\text{-pytz})_4]\cdot NO_3\cdot 2H_2O\}_\infty$ (**7**; 3-Hpytz = 3,5-Di(3-pyridyl)-1,2,4-triazole). A mixture of $Cu(NO_3)_2\cdot 3H_2O$ (0.242 g, 1.0 mmol), aqueous ammonia (25%, 1.0 mL), and 3-cyanopyridine (1.04 g, 10 mmol) was sealed in a 15-mL Teflon-lined reactor and heated in an oven at 100 °C for 60 hrs and slowly cooled to room temperature. The resulting mixture was washed with water, and pale yellow needlelike crystals were collected and dried in air (yield 20−25% based on Cu). Anal. Calcd (%) for $C_{48}H_{36}Cu_5N_{21}O_5$: C, 44.19; H, 2.78; N, 22.55. Found: C, 44.32; H, 2.58; N, 22.64. IR: 3425m, 3064m, 1578m, 1465s, 1419s, 1384m, 1347vs, 1167m, 1106m, 1008m, 817m, 708s cm^{-1}.

$[Cu(4\text{-pytap})_2]$ (**8**; 4-Hpytap = 2,4-Di(4-pyridyl)-1,3,5-triazapentadiene). A mixture of $Cu(OH)_2$ (0.392 g, 4.0 mmol), $(NH_4)_2CO_3$ (0.96 g, 10 mmol), 4-cyanopyridine (1.04 g, 10 mmol), and THF (5.0 mL) was sealed in a 15-mL Teflon-lined reactor and heated in an oven at 90 °C for 60 hrs and slowly cooled to room temperature. The resulting mixture was washed with ethanol, and red platelike crystals were collected and dried in air (yield 10−15% based on Cu). Anal. Calcd (%) for $C_{24}H_{20}CuN_{10}$: C, 56.30; H, 3.94; N, 27.36. Found: C, 56.18; H, 3.81; N, 27.51. IR: 3286s, 3051m, 1575s, 1532vs, 1410s, 1307vs, 995m, 757s cm^{-1}.

$[Ni(4\text{-pytap})_2]$ (**8·Ni**). The reaction was carried out in a method similar to that for **8**, using $Ni_2(OH)_2CO_3$ (0.422 g, 2.0 mmol) instead of $Cu(OH)_2$. However, the temperature can be varied from ca. 90 to 160 °C. The resulting mixture was washed with ethanol, and orange needlelike crystals were collected and dried in air (yield ca. 5% based on Ni). Anal. Calcd (%) for $C_{24}H_{20}NiN_{10}$: C, 56.84; H, 3.97; N, 27.62. Found: C, 56.75; H, 4.03; N, 27.48. IR: 3302s, 3040w, 1600s, 1529vs, 1445vs, 1312vs, 1058m, 844s, 719s cm^{-1}.

$[Ni(4\text{-pytap})_2]\cdot 2H_2O$ (8·Ni·2H$_2$O). A mixture of **8**·Ni (0.051 g, 0.1 mmol) and THF (3.0 mL) was sealed in a 15-mL Teflon-lined reactor and heated in an oven at 120 °C for 60 hrs and slowly cooled to room temperature. The resulting mixture was washed with water, and orange platelike crystals were collected and dried in air (yield ca. 90%). Anal. Calcd (%) for $C_{24}H_{24}N_{10}NiO_2$: C, 53.07; H, 4.45; N, 25.79. Found: C, 53.16; H, 4.39; N, 25.86. IR: 3431s, 3296s, 3031w, 1586vs, 1543vs, 1466vs, 1331vs, 1072m, 946m, 594m cm^{-1}.

$\{[Cu^{II}_3Cu^{I}_6(4\text{-pytap})_6(4\text{-pytz})_2]\cdot 4BF_4\cdot 8H_2O\}_\infty$ (**9**; 4-Hpytz = 3,5-Di(4-pyridyl)-1,2,4-triazole). A mixture of $Cu(OAc)_2\cdot H_2O$ (0.200 g, 1.0 mmol), NH_4BF_4 (0.420 g, 4.0 mmol), 4-cyanopyridine (0.52 g, 5.0 mmol), and absolute ethanol (5.0 mL) was sealed in a 15-mL Teflon-lined reactor and heated in an oven at 95 °C for 6 days and slowly cooled to room temperature. The resulting mixture was washed with ethanol, and red platelike crystals were collected and dried in air (yield less than 5% based on Cu). Anal. Calcd (%) for $C_{96}H_{93}B_4Cu_9F_{16}N_{40}O_8$: C, 40.40; H, 3.28; N, 19.63. Found: C, 40.16; H, 3.05; N, 19.47. IR: 3437s, 3289m, 3023m, 1603vs, 1590s, 1551m, 1430s, 1346m, 993m, 836s, 751m cm^{-1}.

$[Cu_6Cl_3(4\text{-pytz})_3]_\infty$ (**10**). Method A: A mixture of **8** (0.102 g, 0.2 mmol), $CuCl_2\cdot 2H_2O$ (0.170 g, 1.0 mmol), and THF (3.0 mL) was sealed in a 15-mL Teflon-lined reactor and heated in an oven at 120 °C for 60 hrs and slowly cooled to room temperature. Method B: A mixture of $CuCl_2$ (0.268 g, 1.0 mmol), aqueous ammonia (25%, 2.0 mL), and 4-cyanopyridine (1.04 g, 10 mmol) was used rather than that of Method A. The resulting mixture was washed with ethanol, and dark brown crystals were collected and dried in air (yield ca. 80% for method A based on **8**, 20% for method B based on Cu). Anal. Calcd (%) for $C_{36}H_{24}Cu_6Cl_3N_{15}$: C, 37.46; H, 2.10; N, 18.20. Found: C, 37.35; H, 2.22; N, 18.10. IR: 3019w, 1609vs, 1426s, 1017m, 840s, 736m cm^{-1}.

$[Cu_2(OAc)_4(4\text{-pya})_2]$ (**11**; 4-pya = 4-Pyridylamide). The reaction was carried out in a method similar to that for **8**, using $Cu(OAc)_2\cdot H_2O$ (0.200 g, 1.0 mmol) instead of $Cu(OH)_2$. The resulting mixture was washed with THF, and green blocklike crystals were collected and dried in air (yield ca. 15% based on Cu). Anal. Calcd (%) for $C_{20}H_{24}Cu_2N_4O_{10}$: C, 39.54; H, 3.98; N, 9.22. Found: C, 39.45; H, 4.06; N, 9.08. IR: 3326s, 3018m, 2983m, 1618vs, 1590s, 1475s, 1327m, 1133m, 956m, 654m cm^{-1}.

$[Cu(tz)]_\infty$ (**12**; Htz = 1,2,4-Triazole). A mixture of $Cu(NO_3)_2\cdot 3H_2O$ (0.242 g, 1.0 mmol), aqueous ammonia (25%, 2.0 mL), and triazole (0.069 g, 1.0 mmol) was sealed in a 15-mL Teflon-lined reactor and heated in an oven at 160 °C for 60 hrs and slowly cooled to room temperature. The resulting mixture was washed with water, and pale yellow platelike crystals were collected and dried in air (yield 20−25% based on Cu). Anal. Calcd (%) for $C_2H_2CuN_3$: C, 18.25; H, 1.53; N, 31.93. Found: C, 18.15; H, 1.63; N, 31.88. IR: 3130w, 3113w, 1654m, 1494s, 1273s, 1201m, 1151vs, 1054m, 983m, 850m, 666s cm^{-1}.

$[Ag(tz)]_\infty$ (**12·Ag**). A mixture of $AgNO_3$ (0.170 g, 1.0 mmol), aqueous ammonia (25%, 2.0 mL), and triazole (0.069 g, 1.0 mmol) was sealed in a 15-mL Teflon-lined reactor and heated in an oven at 100 °C for 60 hrs and slowly cooled to room temperature. The resulting mixture was washed with ethanol, and colorless crystals were collected and dried in air (yield 50−65% based on Ag). Anal. Calcd (%) for $C_2H_2AgN_3$: C, 13.65; H, 1.15; N, 23.89. Found: C, 13.60; H, 1.22; N, 23.77. IR: 3125w, 3101w, 1650m, 1494s, 1273s, 1201m, 1151vs, 1054m, 983m, 850m, 666s cm^{-1}.

X-ray Crystallography. Diffraction intensities were collected on a Bruker Apex CCD area-detector diffractometer (Mo Kα, λ 0.71073 Å). Absorption corrections were applied by using multiscan program SADABS.[32] The structures were solved with direct methods and refined with a full-matrix least-squares technique with the SHELXTL program package.[33] Anisotropic thermal parameters were applied to all non-hydrogen atoms. The organic hydrogen atoms were generated geometrically (C−H 0.96 Å); the aqua hydrogen atoms were located from difference maps and refined with isotropic temperature factors. Crystal data as well as details of data collection and refinements for the complexes are summarized in Table 1. The CCDC contains the supplementary crystallographic data for this article. These data can be obtained free of charge via http://www.ccdc.cam.ac.uk/conts/retriev-

(32) Sheldrick, G. M. *SADABS 2.05*; University of Göttingen: Göttingen, Germany.
(33) *SHELXTL 6.10*; Bruker Analytical Instrumentation: Madison, WI, 2000.

Table 1. Crystallographic Data and Structure Refinements[a]

compd	**1**[b]	**2**	**3**[b]	**4**	**5**
formula	$C_4H_6CuN_3$	$C_6H_{12}CuN_3O$	$C_8H_{14}CuN_3$	$C_{41}H_{72}Cu_5N_{13}$	$C_{84}H_{60}Cu_6N_{18}$
FW	159.66	205.73	431.52	1064.82	1702.74
space group	$P4_2/n$ (No. 86)	$Im\bar{3}$ (No. 204)	$Im\bar{3}$ (No. 204)	$Fdd2$ (No. 43)	$P2_1/n$ (No. 14)
a/Å	13.470(2)	14.9159(7)	14.923(2)	43.733(5)	15.7158(6)
b/Å	13.470(2)	14.9159(7)	14.923(2)	26.579(3)	21.8620(8)
c/Å	6.142(2)	14.9159(7)	14.923(2)	39.339(4)	23.7775(9)
α/deg	90	90	90	90	90
β/deg	90	90	90	90	108.778(8)
γ/deg	90	90	90	90	90
V/Å^3	1114.6(5)	3318.6(3)	3323.2(8)	45726(8)	7734.6(6)
Z	8	12	12	32	4
D_c/g cm^{-3}	1.903	1.236	1.294	1.237	1.462
T/K	293(2)	123(2)	293(2)	123(2)	293(2)
μ/mm^{-1}	3.796	1.934	1.928	1.867	1.677
R_1 ($I > 2\sigma$)	0.0237	0.0531	0.0477	0.0820	0.0575
wR_2 (all data)	0.0646	0.1572	0.1516	0.2109	0.1886
GOF	1.082	0.997	1.154	1.047	1.035

compd	**6**	**7**	**8**	**8**·Ni	**8**·Ni·2H$_2$O
formula	$C_{60}H_{44}Cu_4N_{22}O_6$	$C_{48}H_{36}Cu_5N_{21}O_5$	$C_{24}H_{20}CuN_{10}$	$C_{24}H_{20}N_{10}Ni$	$C_{24}H_{24}N_{10}NiO_2$
FW	1423.33	938.86	512.05	507.19	543.24
space group	$P\bar{1}$ (No. 2)	$P2/c$ (No. 13)	$C2/c$ (No. 15)	$C2/c$ (No. 15)	$P\bar{1}$ (No. 2)
a/Å	10.4237(9)	17.4879(11)	17.4349(9)	17.4679(8)	6.9193(10)
b/Å	12.6458(10)	12.5107(8)	7.1639(4)	6.9798(3)	9.4382(13)
c/Å	13.6176(11)	21.5927(13)	18.6729(10)	19.2699(9)	9.7675(14)
α/deg	67.5390(10)	90	90	90	81.852(3)
β/deg	71.2250(10)	93.6040(10)	110.8430(10)	112.3320(10)	73.411(3)
γ/deg	67.0000(10)	90	90	90	82.154(3)
V/Å^3	1495.2(2)	4714.8(5)	2179.7(2)	2173.2(2)	602.04(15)
Z	1	4	4	4	1
D_c/g cm^{-3}	1.581	1.838	1.560	1.550	1.498
T/K	293(2)	293(2)	123(2)	123(2)	123(2)
μ/mm^{-1}	1.476	2.295	1.039	0.930	0.851
R_1 ($I > 2\sigma$)	0.0469	0.0552	0.0296	0.0310	0.0349
wR_2 (all data)	0.1284	0.1504	0.0822	0.0813	0.0910
GOF	1.020	1.016	1.052	1.026	1.046

compd	**9**	**10**	**11**	**12**	**12**·Ag
formula	$C_{96}H_{93}B_4Cu_9F_{16}N_{40}O_8$	$C_{36}H_{24}Cl_3Cu_6N_{15}$	$C_{20}H_{24}Cu_2N_4O_{10}$	$C_2H_2CuN_3$	$C_2H_2AgN_3$
FW	2854.16	1154.35	607.51	131.61	175.94
space group	$P2_1/n$ (No. 14)	$Fdd2$ (No. 43)	$P2_1/c$ (No. 14)	$P\bar{1}$ (No. 2)	$P\bar{1}$ (No. 2)
a/Å	20.4436(13)	31.667(2)	10.4549(8)	8.0017(7)	8.1270(6)
b/Å	16.9489(11)	10.4902(7)	13.4937(10)	8.5956(7)	8.7159(7)
c/Å	23.1265(15)	21.2886(15)	8.6815(7)	10.5915(9)	11.4385(9)
α/deg	90	90	90	79.648(4)	80.177(4)
β/deg	112.0070(10)	90	100.579(2)	79.043(3)	79.310(6)
γ/deg	90	90	90	78.855(4)	84.147(6)
V/Å^3	7429.4(8)	7071.9(8)	1203.93(16)	693.94(10)	782.43(11)
Z	2	8	2	8	8
D_c/g cm^{-3}	1.276	2.168	1.676	2.520	2.987
T/K	220(2)	123(2)	220(2)	293(2)	293(2)
μ/mm^{-1}	1.337	3.828	1.829	6.067	4.952
R_1 ($I > 2\sigma$)	0.0590	0.0298	0.0379	0.0328	0.0250
wR_2 (all data)	0.2267	0.0670	0.0981	0.0934	0.0637
GOF	1.041	1.005	1.032	1.064	1.050

[a] $R_1 = \sum||F_o| - |F_c||/\sum|F_o|$, $wR_2 = [\sum w(F_o^2 - F_c^2)^2/\sum w(F_o^2)^2]^{1/2}$. [b] See ref 12.

ing.html (or from the Cambridge Crystallographic Data Centre, 12 Union Road, Cambridge CB21EZ, U.K.; fax:(+44) 1223-336-033).

Results and Discussion

Synthesis and Ligand Formation Mechanism. Treatments of various organonitriles such as alkyl nitriles, phenyl nitriles, and pyridyl nitriles incorporating with Cu^{II} and ammonia under solvothermal conditions afford corresponding 3,5-disubstituted 1,2,4-triazolates, which are coordinated to the Cu^{II} or reduced Cu^{I} ions to afford crystalline materials. The triazoles can only be obtained when the Cu^{II} salts were used and the reaction temperature is higher than 100 °C. Since ammonia may also be generated from the hydrolysis of nitriles, we carried out these reactions at different pH values by addition of aqueous acid or base rather than aqueous ammonia, but no triazole could be detected when T < 180 °C. Therefore, we believe that the triazolates were derived from the coupling of nitriles and ammonia in 2:1 molar ratio, and the Cu^{II} ions should act as an oxidant during the multistep formation of the triazolato ring. Scheme 1 shows one-pot formation of triazolates under solvothermal conditions.

On the basis of the literature, several possible mechanisms should be addressed: (I) the diazabutadiene-1,4-diamine, (II) the 1,3,5-triazapentadiene, and (III) the dicopper site routes

Scheme 1. One-Pot Formation of Triazolates under Solvothermal Condition

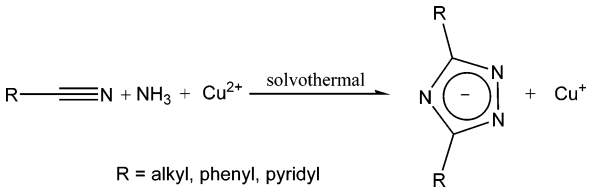

Scheme 2. Selected Possible Reaction Mechanisms

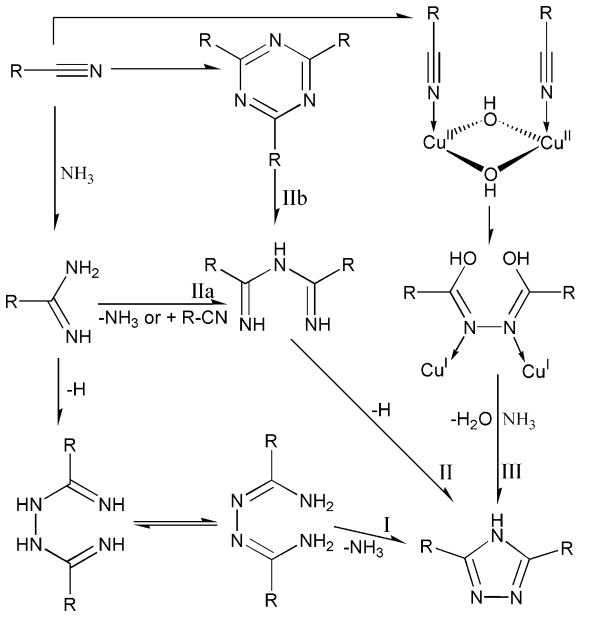

(Scheme 2). Diazabutadiene-1,4-diamine can rapidly lose NH_3 to form the triazole, and this diamine intermediate can be generated by oxidative coupling of amidine (I).[34] Amidine was also known to couple or add to another nitrile to give 1,3,5-triazapentadiene,[19,20] which may further undergo a two-electron oxidative cyclization to form the triazole (IIa). The 1,3,5-triazapentadiene can also be decomposed from 1,3,5-triazine,[21] which can be generated from the trimerization of nitrile molecules (IIb).[27] However, the route IIb may be excluded since no ammonia is needed for its formation. While pursuing the possible reaction mechanism, we came across another example concerned with in situ generation of 1,2,4-triazoles from nitriles (dicopper site route III).[23] A dinuclear copper(I) complex, "wet" nitrile solvents, and dioxygen atmosphere, but no additional ammonia, were required for this reaction. The authors suggested that the N−N bond is coupled from two nitriles on the dimetal site prior to the ring closure, which is promoted by condensation between NH_3 and hydroxyl groups (the N atom from NH_3 is fixed at the 4-position).

The NH_3 required for the reactions was suggested to be generated from the hydrolysis of the nitriles in previous examples.[27] It should be noted that no experiment involving the external addition of NH_3 was carried out, although the hydrolysis causes the obviously uneconomic consumption of nitrile. Except route II, the N−N bonds are formed before the formation of triazolato ring, which is related to the traditional preparation of 1,2,4-triazoles from hydrazine derivatives.[6,35]

One should be aware that only a few of the possible mechanisms have been mentioned above for the reaction versatility of the organonitriles. In addition, investigation of the mechanism is further prohibited as the reactions involve rather volatile reactants and only occur at relatively high temperature and pressure. Some intermediates would also be hydrolyzed and/or decomposed in aqueous medium.[20,27] However, some of the proposed intermediates may be trapped and stabilized by complexation with metal ions in crystalline state via complexation with metal ions or supramolecular interactions, if we could properly select and control the reaction temperature, time, and medium.

Attempting to answer the above questions, we synthesized and structurally characterized by X-ray crystallography various metal complexes exhibiting related solvothermal metal/ligand reactions and/or novel coordination structures (Table 2).

Our persistent attempt was successful when the reaction was carried out in THF at 90 °C and used $(NH_4)_2CO_3$ as a source of ammonia. Solvothermal reaction of $Cu(OH)_2$, $(NH_4)_2CO_3$, and 4-cyanopyridine in THF afforded the 1,3,5-triazapentadiene intermediate, neutral $[Cu^{II}(4\text{-pytap})_2]$ (**8**, 4-Hpytap = 2,4-di(4-pyridyl)-1,3,5-triazapentadiene), without solvate. The Cu^{II} center in **8** is chelated by two bidentate 4-pytz ligands to furnish a square-planar coordination environment (Figure 1). The Cu−N bond lengths (1.941(1) and 1.954(1) Å) and the two corner-sharing planar six-membered metallocycles as well as the unusual red color of crystalline **8** are similar to those of relevant Cu^{II} bis-1,3,5-triazapentadienates, in which the ligands were generated from decomposition of the 1,3,5-triazines[21] or coupling between dicyanoamide and methanol (or pyrazole).[22] Although Ni^{II} complexes bearing similar anionic or neutral ligands have been well-studied, **8** represents the first example of Cu^{II}-mediated synthesis of 1,3,5-triazapentadiene from nitrile and ammonia. The 1,3,5-triazapentadienates in these Ni^{II} complexes can be prepared either by self-condensation of acetamidine,[36] reactions between nitriles and highly reactive $LiN(SiMe_3)_2$,[37] or nitriles and wet solvents catalyzed by dinickel complexes[19] or oximes.[20] We also obtained orange $[Ni(4\text{-pytap})_2]$ (**8**·Ni) by use of $Ni_2(OH)_2CO_3$ as the starting materials under reaction conditions similar to those used for the isostructural **8**. The Ni−N bond lengths (1.859(1), 1.867(1) Å) are significantly shorter than those in Cu^{II} analogues but comparable to the other Ni^{II} analogues (see Figure S1 in Supporting Information).[19,20,36,37] However, it should be noted that synthesis of other analogues by use of Co^{II} or Zn^{II} salts or other nitriles is not successful. We therefore believe that the square-planar coordination behavior of Cu^{II} and Ni^{II} is crucial for stabilization of these Cu^{II} and Ni^{II} complexes. The 4-pyridyl groups were also involved in multiple intermolecular N−H···N hydrogen bonds and $\pi-\pi$ interactions, which may promote the crystallization of **8** and **8**·Ni from the reaction mediums. Actually, discrete **8** and **8**·Ni are virtually insoluble in THF and common organic solvents.

A mixed-valence complex $\{[Cu^{II}_3Cu^{I}_6(4\text{-pytap})_6(4\text{-pytz})_2]\cdot 4BF_4\cdot 8H_2O\}_\infty$ (**9**, 4-Hpytz = 3,5-di(4-pyridyl)-1,2,4-triazole)

(34) Kauffmann, T.; Albrecht, J.; Berger, D.; Legler, J. *Angew. Chem., Int. Ed.* **1967**, *6*, 633−634.

(35) (a) El Ashry, E. S. H.; Awad, L. F.; Winkler, M. *J. Chem. Soc., Perkin Trans. 1* **2000**, 829−834. (b) Liu, C.-J.; Iwanowicz, E. J. *Tetrahedron Lett.* **2003**, *44*, 1409−1411.

(36) Norrestam, R. *Acta Crystallogr., Sect. C* **1984**, *40*, 955.

(37) Guo, J.-P.; Wong, W.-K.; Wong, W.-Y. *Eur. J. Inorg. Chem.* **2004**, 267−275.

Table 2. Solvothermal Metal/Ligand Reactions and Structure Descriptions of the Metal Complexes[d]

compd	formula	product (reactant) of the metal/ligand reaction	coordination structure
1	$[Cu(mtz)]_\infty$	Cu^I (Cu^{II}), mtz (acetonitrile)[a]	3-connected 4.8.16 net or 4-connected $4^2 8^4$ net
2	$\{[Cu(etz)]\cdot H_2O\}_\infty$	Cu^I (Cu^{II}), etz (propionitrile)[a]	3-connected 4.12^2 net or 4-connected NbO net
3	$[Cu(ptz)]_\infty$	Cu^I (Cu^{II}), ptz (butyronitirle)[a]	3-connected 4.12^2 net or 4-connected NbO net
4	$[Cu_5CN(btz)_4]_\infty$	Cu^I (Cu^{II}), btz and CN (valeronitrile)[a]	3D network with mixed 3- and 4-connected centers
5	$[Cu_6(phtz)_6]_\infty$	Cu^I (Cu^{II}), phtz (benzonitrile)[a]	1D zigzag chain based on pentanuclear clusters
6	$[Cu^I_2Cu^{II}_2(2\text{-pytz})_4(2\text{-pa})_2]\cdot 2H_2O$	Cu^I (Cu^{II}), 2-pytz and 2-pa (2-cyanopyridine)[a]	0D
7	$\{[Cu_5(3\text{-pytz})_4]\cdot NO_3\cdot 2H_2O\}_\infty$	Cu^I (Cu^{II}), 3-pytz (3-cyanopyridine)[a]	2D cationic network
8	$[Cu(4\text{-pytap})_2]$	4-pytap (4-cyanopyridine)[b]	0D
8·Ni	$[Ni(4\text{-pytap})_2]$	4-pytap (4-cyanopyridine)[b]	0D
8·Ni·$2H_2O$	$[Ni(4\text{-pytap})_2]\cdot 2H_2O$		0D
9	$\{[Cu^{II}_3Cu^I_6(4\text{-pytap})_6(4\text{-pytz})_2]\cdot 4BF_4\cdot 8H_2O\}_\infty$	Cu^I (Cu^{II}), 4-pytap and 4-pytz (4-cyanopyridine)[c]	3D cationic network
10	$[Cu_6Cl_3(4\text{-pytz})_3]_\infty$	Cu^I (Cu^{II}), 4-pytz (4-pytap)	complicated 3D network
11	$[Cu_2(OAc)_4(4\text{-pya})_2]$	4-pya (4-cyanopyridine)[b]	0D
12	$[Cu(tz)]_\infty$	Cu^I (Cu^{II})	3-connected 4.8^2 net or 4-connnected (4,4) net
12·Ag	$[Ag(tz)]_\infty$		3-connected 4.8^2 net or 4-connnected (4,4) net

[a] Using aqueous ammonia as the ammonia source. [b] Using ammonium carbonate as the ammonia source. [c] Using NH_4BF_4 as the ammonia source [d] Htz = 1,2,4-triazole, Hmtz = 3,5-dimethyl-1,2,4-triazole, Hetz = 3,5-diethyl-1,2,4-triazole, Hptz = 3,5-dipropyl-1,2,4-triazole, Hbtz = 3,5-dibutyl-1,2,4-triazole, Hphtz = 3,5-diphenyl-1,2,4-triazole, 2-Hpytz = 3,5-di(2-pyridyl)-1,2,4-triazole, 3-Hpytz = 3,5-di(3-pyridyl)-1,2,4-triazole, 4-Hpytz = 3,5-di(4-pyridyl)-1,2,4-triazole, 2-Hpa = pyridine-2-carboxylic acid, 4-Hpytap = 2,4-di(4-pyridyl)-1,3,5-triazapentadiene, 4-pya = 4-pyridylamide, HOAc = acetic acid.

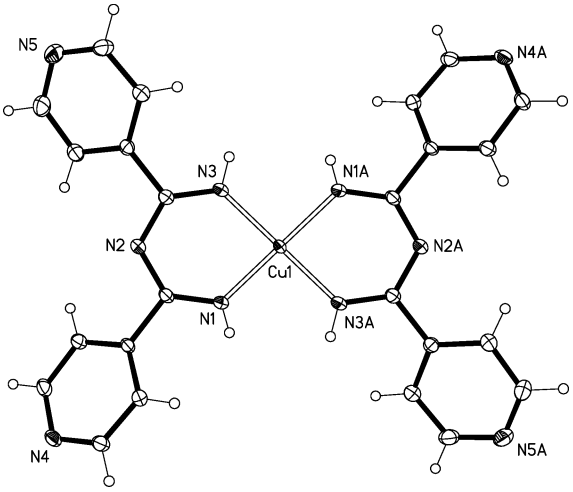

Figure 1. Molecular structure of **8** (thermal ellipsoids: 50%; A: $-x$, $1-y$, $1-z$).

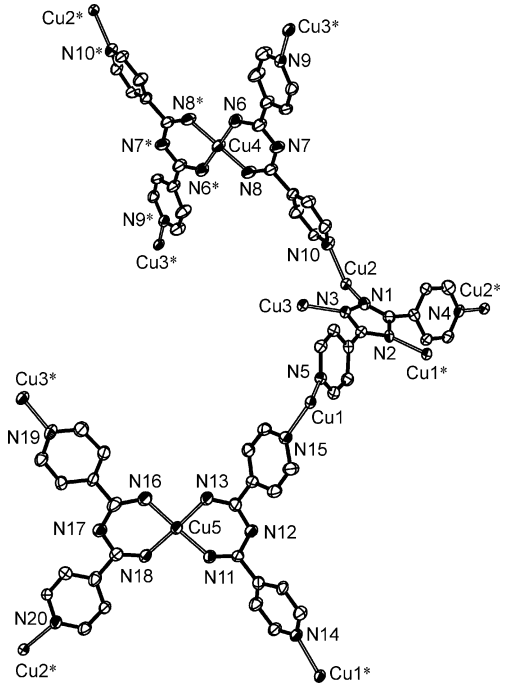

Figure 2. Perspective view of coordination environments of the 4-pytap and 4-pytz ligands in **9** (thermal ellipsoids: 50%; hydrogen atoms are omitted for clarity; * symmetrically generated).

containing both 1,3,5-triazapentadienate and 1,2,4-triazolate ligands has also been isolated in very low yield when $Cu(OAc)_2\cdot 2H_2O$ and NH_4BF_4 were used. The asymmetric unit of **9** contains one and a half Cu^{II} and three Cu^I centers, three 4-pytap and one 4-pytz ligands. The square-planar Cu^{II} coordination environments (Cu−N 1.893(4)−1.962(5) Å) in **9** are similar to that in **8**, while the $Cu^{II}(4\text{-pytz})_2$ fragments behave as exo-tetradentate metalloligands with all of the four pyridyl ends coordinated to the Cu^I centers. All of the five nitrogen donors of the anionic 4-pytz are coordinated to different Cu^I centers, which adopt trigonal (Cu−N 1.913(4)−2.079(5) Å) or tetrahedral (Cu−N 2.020(4)−2.079(4) Å) geometries (Figure 2). The infinite structure of **9** contains $[Cu^I(4\text{-pytz})]_\infty$ ribbonlike fragments, which are connected by two pyridyl groups of the $Cu^{II}(4\text{-pytap})_2$ metalloligands to form sheets. These sheets further interlinked to give a 3D porous cationic network via the coordination bonds between Cu^I and the remaining pyridyl groups in an ABCABC··· fashion (see Figure S2 in Supporting Information). It should be noted that the reaction time required for **9** was rather long (6 days), and the low yield may be due to the relatively low pH and higher stability of NH_4BF_4. In contrast, $(NH_4)_2CO_3$ and $Cu(OH)_2$ in the synthesis of **8** can release free ammonia and promote the deprotonation of the ligands easier.

To further verify whether the 1,3,5-triazapentadiene ligands are really the intermediates, we also tried to synthesize the final 3,5-di(4-pyridyl)-1,2,4-triazole by using **8** and **8**·Ni as starting

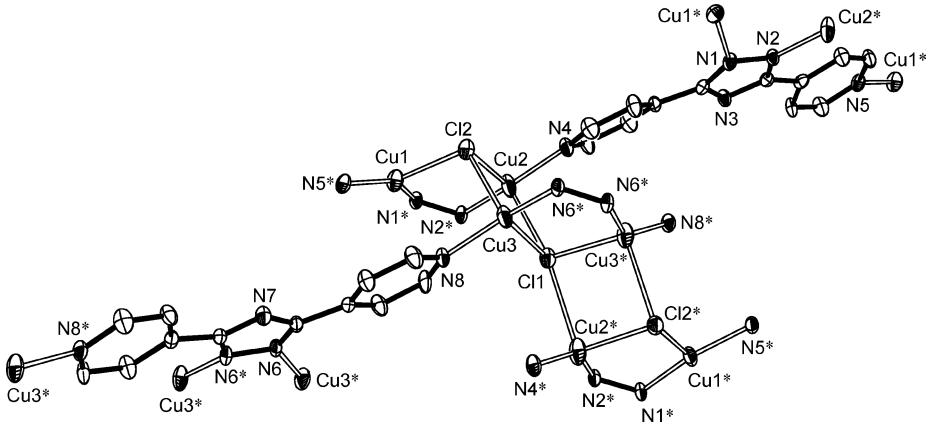

Figure 3. Perspective view of coordination environments of **10** (thermal ellipsoids: 50%; hydrogen atoms are omitted for clarity; * symmetrically generated).

materials. **8**·Ni is very stable under the solvothermal treatment up to 160 °C in THF, giving only a new dihydrate [Ni(4-pytap)$_2$]·2H$_2$O (**8**·Ni·2H$_2$O, see Figure S3 in Supporting Information) in excellent yield. However, **8** could be converted into yellow powders in ca. 20% yield at 120 °C. Microanalysis of these yellow powders agreed well with the [Cu^I(4-pytz)] composition (calcd: C, 50.43; H, 2.82; N, 24.51; found: C, 50.56; H, 2.97; N, 24.36). Additional Cu^{II} sources were also introduced into these trials, and most resulted in similar observations, while the addition of CuCl$_2$·2H$_2$O (with quantity larger than the requirement of two Cu^{II} ions per 4-pytap) gave deep brown crystals ([Cu$_6$Cl$_3$(4-pytz)$_3$]$_\infty$ (**10**) from **8** in high yield (ca. 80% based on **8**) and from **8**·Ni in moderate yield (ca. 50% based on **8**·Ni). Single-crystal X-ray analysis of **10** revealed a 3D metal−organic structure composed of unusual μ_3- and μ_4-Cl bridged Cu$_6$Cl$_3$ clusters (Cu−Cl 2.431(1)−2.586(1) Å) and μ_4-coordinating 4-pytz ligands (except the 4-positions of triazolate) (Figure 3). The Cu$_6$Cl$_3$ clusters are extended to metal−organic ribbons via coordination of the 4-pytz pyridyl ends, which are further interlinked to the final 3D network through interation between Cu^I and the remaining 4-pytz pyrazolate sites (Cu−N 1.923(3)−1.980(3) Å) (see Figure S4 in Supporting Information).

There is no proposed intermediate for route I, IIb, or III isolated in crystalline form or detected from the ESI-MS. Although no amidine intermediate was isolated or detected, we did isolate the free amide[31] and a Cu^{II} complex of 4-pyridylamide [Cu$_2$(OAc)$_4$(4-pya)$_2$], (**11**, 4-pya = 4-pyridylamide, the molecular structure depicted in Figure S5 in Supporting Information). The amide byproduct may be derived directly from the hydrolysis of nitriles or from the amidines. The syntheses of amidine from nitrile and ammonia[27] and 1,3,5-triazapentadiene from amidine have also been reported to be mediated by metal ions.[36] Therefore, the most reasonable mechanism for our reactions should be route IIa: Cu^{II}-ligated RCN is first attacked by NH$_3$ to form amidine, which further self-condenses or reacts with another RCN to form Cu^{II}-ligated 1,3,5-triazapentadiene. These two steps can also be promoted by Ni^{II}. The 1,3,5-triazapentadiene offers another coordination site for the second Cu^{II} cation after deprotonation. In the final step, 1,3,5-triazapentadienate loses two protons and then transfers two electrons to the Cu^{II} centers (Cu^{II} → Cu^I) to form the N−N bond (Scheme 3). High pH is favored for the deprotonation in the last two steps, which is in good agreement with our observations. This mechanism is remarkable since most 1,2,4-

Scheme 3. Proposed Ligand Formation Mechanism under Solvothermal Condition

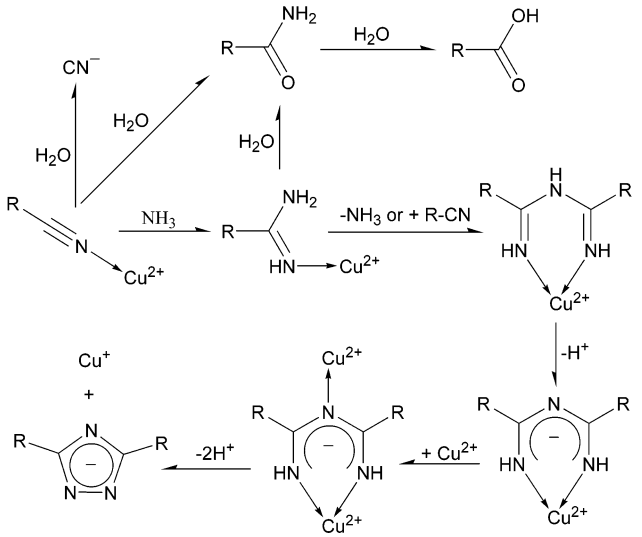

triazoles were prepared in several steps involving the use of hydrazine derivatives or conversion of other ring systems containing N−N bonds.[6,35] In particular, the hydrazine and its derivatives must be first prepared from ammonia.[38]

In our trials, only crystals in good quality were collected, and the overall yields of the triazolates were relatively low. However, one should notice that the theoretical yields of our reactions should be less than 100% based on the copper sources since every two Cu^{II} can produce only one triazolate. By considering organonitrile as a versatile reagent in many reactions, it may be transferred to some undesired byproducts such as carboxylic acids in the aqueous medium.[24,25] A tetranuclear Cu^{I,II} complex bearing both 3,5-di(2-pyridyl)-1,2,4-triazolates and pyridine-2-carboxylates [Cu$^I_2$Cu$^{II}_2$(2-pytz)$_4$(2-pa)$_2$]·2H$_2$O (**6**, 2-Hpytz = 3,5-di(2-pyridyl)-1,2,4-triazole, 2-Hpa = pyridine-2-carboxylic acid) was isolated in low yield at low temperature as a byproduct of the tetranuclear [Cu$^I_4$(2-pytz)$_4$], which is one of the four supramolecular isomers of binary Cu^I 3,5-di(2-pyridyl)-1,2,4-triazolate.[31] The new 1:1 mixed valent **6** should be regarded as a two-electron oxidized product of [Cu$^I_4$(2-pytz)$_4$]. The two Cu^{II} centers were further chelated by pyridine-2-carboxylates to accomplish elongated octahedral coordination spheres, while the two Cu^I centers retain distorted tetrahedral

(38) Ragnarsson, U. *Chem. Soc. Rev.* **2001**, *30*, 205−213.

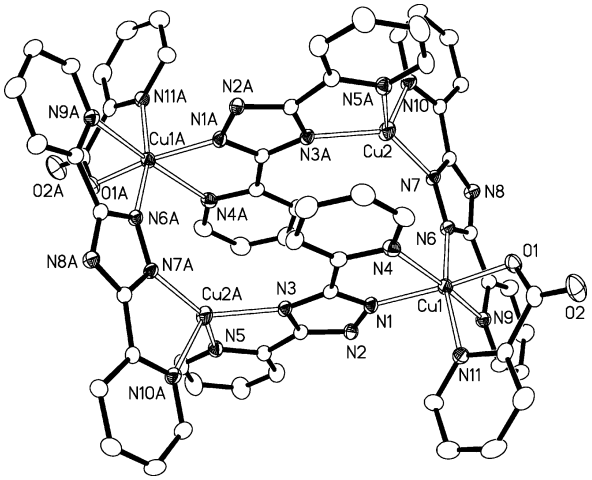

Figure 4. Molecular structure of **6** (thermal ellipsoids: 30%; hydrogen atoms are omitted for clarity; A: $-x, 1-y, 1-z$). Selected bond lengths: Cu1−O1 1.997(3), Cu1−N1 2.003(3), Cu1−N4 2.456(4), Cu1−N6 1.978(3), Cu1−N9 2.420(4), Cu1−N11 2.026(3), Cu2−N7 1.970(3), Cu2−N10 2.170(3) Å.

environments (Figure 4). The carboxylic acid "byproduct" was suggested in other related reactions to account for the origin of the ammonia;[19,20,23] however, it may be only regarded as a byproduct in our reaction.

When valeronitrile was used as a starting organonitrile, a 3D metal−organic network $[Cu_5CN(btz)_4]_\infty$ (**4**, Hbtz = 3,5-dibutyl-1,2,4-triazole) was obtained. It contains not only the desired triazolate but also the unexpected cyanide ligands. The Cu^I centers in **4** adopt linear, trigonal, and tetrahedral coordination environments, while the triazolates and cyanides were all in μ_3 and μ_2 coordination modes, respectively (see Figure S6 in Supporting Information). The C−C bond cleavage of nitriles to cyanide is mediated by metal complexes under ambient or solvothermal conditions.[13,24]

Topologies of Cu(I) Triazolates. The ligand reaction products, 1,2,4-triazoles, are good candidates for the construction of coordination architectures since they exhibit the coordination modes of both pyrazoles and imidazoles. It has been known that the highly predictable coordination modes of the imidazolates promoted the rational design of 0D and 1D structures with univalent metal centers and 4-connected networks with divalent metal centers.[9−11] From the topological point of view, univalent metal centers (Cu^I and Ag^I) and triazolates should be more important since they can be used to construct the simplest 3-connected networks in the most straightforward way. However, no crystal structure of a binary metal triazolate has been reported before our work.[12] The simple binary $[Cu(mtz)]_\infty$ (**1**, Hmtz = 3,5-dimethyl-1,2,4-triazole) and $[Cu(ptz)]_\infty$ (**3**, Hptz = 3,5-dipropyl-1,2,4-triazole) represent the first examples of the 3-connected nets 4.8.16 and 4.12^2, respectively (see Figure S7 and S8 in Supporting Information), as described in our previous communication.[12] A variety of intriguing 3-connected nets were predicted by Wells a few decades ago,[1] but most of them have rarely met the true examples in the context of coordination chemistry.[39] The 3-connected 4.8.16 and 4.12^2 nets can also be regarded as 4-connected 4^28^4 (long Schläfli symbol $4.4.8_4.8_4.8_8.8_8$) and NbO nets, respectively, two of the few nets solely constructed by square-planar nodes.[40] The differences among the 3D 4^28^4, NbO, and related 2D (4,4) (can be also augmented to 3-connected 4.8^2) nets are the dihedral angles between the adjacent nodes, that is, parallel for (4,4), acute for 4^28^4,[40d] and perpendicular for NbO.[40a] The rational design of the 3D 4^28^4 or NbO topologies rather than the 2D (4,4) ones is highly appreciated for the purpose of porous materials.[40] But few examples have been reported to have the 3D 4^28^4 or NbO net since the 2D (4,4) net was commonly encountered when square-planar building blocks were used. The strategy of controlling the dihedral angles has been successfully used in a several recent reports, in which the dihedral angles between adjacent rigid square-planar SBUs are determined by the ligands with predesigned geometries.[4c] In the cases of **1** and **3**, the dihedral angles are determined by a rather different way (repulsion between adjacent square-planar nodes), as there is no ligand acting as the linear linkers. The (4,4), 4^28^4, and NbO nets should be regarded as the simplest ones in the context of 4-connected nets based solely on square-planar nodes as they have only one type of dihedral angle between adjacent nodes. On the other hand, other known 4-connected nets based solely on square-planar nodes (i.e., the $CdSO_4$[40b] and USF-1[40f] nets) are more complicated as they contain two types of dihedral angles between adjacent nodes. Therefore, we may rationally construct these three simple but important nets (**A** for (4,4) or 4.8^2, **B** for 4^28^4 or 4.8.16, **C** for NbO or 4.12^2) via alteration of the sizes of the substituents of the triazolates (Scheme 4).

According to the above analyses, a planar net **A** for the Cu^I triazlates could only be synthesized when the substitutent was smaller than the methyl group (e.g., the unsubstituted triazole). Although most examples of nets **B** or **C** are porous, **1** and **3** are nonporous materials due to the 2-fold interpenetration and the bulky propyl groups, respectively. However, we can predict the Cu^I 3,5-diethyl-1,2,4-triazolate to have a porous **B** or **C** structure as the ethyl groups can exclude the interpenetration of the **B** net or retain the cavities of the **C** net, respectively.

X-ray analysis of $\{[Cu(etz)]\cdot H_2O\}_\infty$ (**2**, Hetz = 3,5-diethyl-1,2,4-triazole) revealed cell parameters identical to those of **3**, indicating that **2** and **3** are **C** net of isostructural architectures. As expected, **2** is highly porous and the potential solvent accessible areas are calculated to be ca. 40% of the total crystal volume.[41] The cavities in **2** are occupied by water molecules. The low site occupancy for the disordered water molecules can be attributed to the hydrophobic nature of the host, and the crystalline prisms of **2** rapidly lose the guests and the crystal is efflorescent under ambient conditions. The open framework of **2** is indicated by the spherical voids with diameter of ca. 9 Å, and the volume of the van der Waals sphere that fits inside the voids is ca. 400 $Å^3$ (Figure 5). Similar to the case of the propyl groups in **3**, flexible ethyl groups in **2** are also disordered in the lattice, which can be considered as the terminal methyl groups rotating along the C−C bonds. Therefore, apertures of

(39) (a) Abrahams, B. F.; Batten, S. R.; Grannas, M. J.; Hamit, H.; Hoskins B. F.; Robson, R. *Angew. Chem., Int. Ed.* **1999**, *38*, 1475−1477. (b) Abrahams, B. F.; Jackson, P. A.; Robson, R. *Angew. Chem., Int. Ed.* **1998**, *37*, 2656−2659. (c) Carlucci, L.; Ciani, G.; Proserpio, D. M.; Rizzato, S. *Chem. Commun.* **2001**, 1198−1199.

(40) (a) Eddaoudi, M.; Kim, J.; O'Keeffe, M.; Yaghi, O. M. *J. Am. Chem. Soc.* **2002**, *124*, 376−377. (b) Barnett, S. A.; Blake, A. J.; Champness, N. R.; Wilson, C. *Chem. Commun.* **2002**, 1640−1641. (c) Carlucci, L.; Ciani, G.; Macchi, P.; Proserpio, D. M. *Chem. Commun.* **1998**, 1837−1838. (d) Rather, B.; Moulton, B.; Walsh, R. D. B.; Zaworotko, M. J. *Chem. Commun.* **2002**, 694−695. (e) Carlucci, L.; Cozzi, N.; Ciani, G.; Moret, M.; Proserpio, D. M.; Rizzato, S. *Chem. Commun.* **2002**, 1354−1355. (f) Moulton, B.; Abourahma, H.; Bradner, M. W.; Lu, J.-J.; McManus, G. J.; Zaworotko, M. J. *Chem. Commun.* **2003**, 1342−1343.

(41) Spek, A. L. *PLATON*, Utrecht University: Utrecht, The Netherlands, 2003.

Scheme 4. Relationship of the Dihedral Angles and the Substituents in the $[Cu(tz)]_\infty$ Featuring $Cu_2(tz)_2$ Building Blocks with Only a Difference in the Substituents[a]

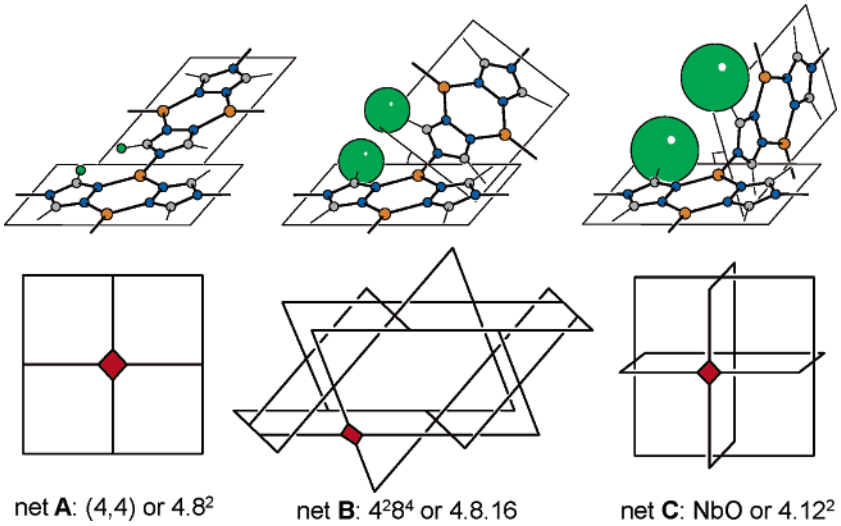

[a] Orange, copper; blue, nitrogen; gray, carbon. Only a pair of substituents is highlighted in green for clarity; red squares indicate the augmentation of 3-connected nets from corresponding 4-connected nets.

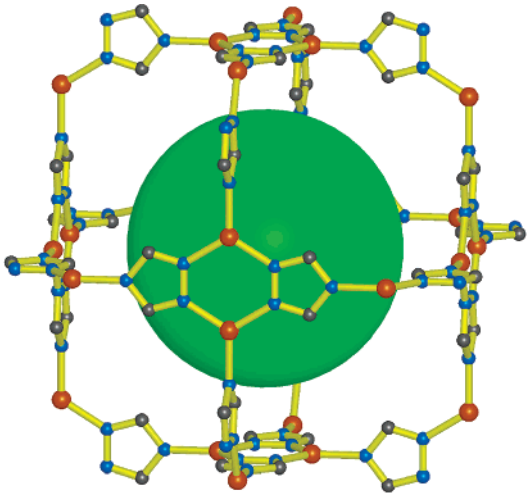

Figure 5. Perspective view of an NbO cage of **2** (substituents and guest molecules are omitted for clarity; orange, copper; blue, nitrogen; gray, carbon; green, internal void; Cu···Cu 3.448(6) Å; Cu−N 1.960(4)−1.962(4) Å; N−Cu−N 116.4(2)−121.8(2)°).

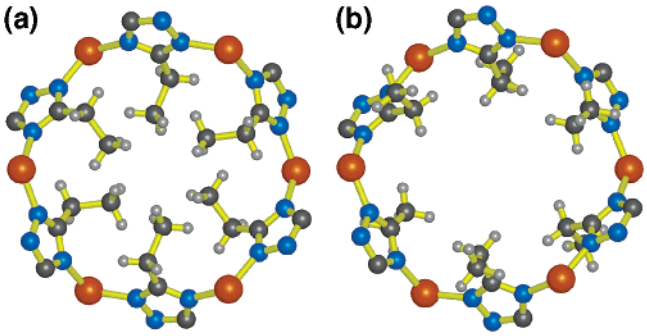

Figure 6. Closed (a) and opened (b) states of the hexagonal windows in the porous network **2**.

the cavity in **2** may be regarded as "operable" windows, which can be opened or closed by the rotation of the terminal methyl groups (Figure 6).

Since the unsubstituted triazole cannot be obtained from our in situ reactions, the Cu^I triazolate $[Cu(tz)]_\infty$ was directly

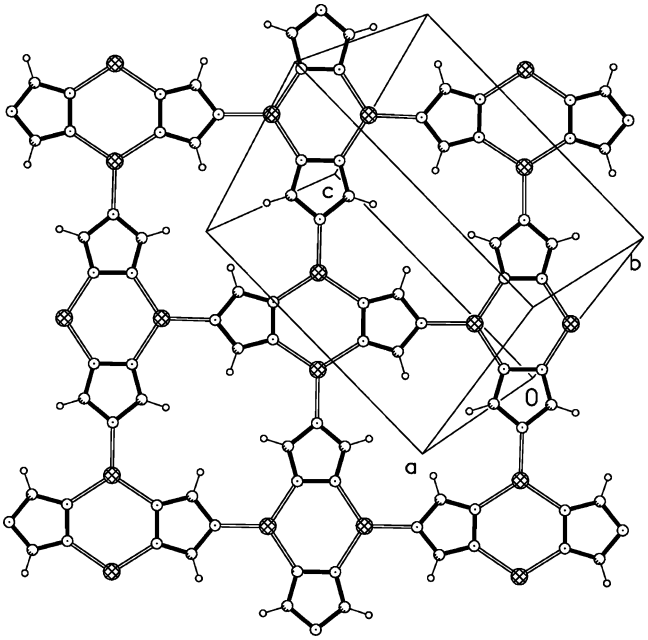

Figure 7. Perspective view of the 2D network in **12**.

synthesized using commercially available triazole and Cu^{II} salts by methods similar to those used for preparing Cu^I or $Cu^{I,II}$ imidazolates.[10] Crystalline product $[Cu(tz)]_\infty$ (**12**, Htz = 1,2,4-triazole) was isolated and structurally characterized as the predicted net **A**. Despite the simple composition, the asymmetric unit of **12** contains four Cu(tz) moieties, featuring similar configurations with its analogues (Cu···Cu 3.531(4)−3.532(4) Å, Cu−N 1.941(3)−1.988(3) Å, N−Cu−N 113.2(1)−125.0(1)°). The 2D network of **12** matches the (110) family of planes and provides potential $\pi\cdots\pi$, Cu···π, and Cu···Cu (3.148, 3.316, 3.457, 3.503 Å) interactions for crystal packing (Figure 7).[30] The very short average plane-to-plane separation 3.105 Å in **12** is noteworthy (see Figure S9 in Supporting Information), and a shorter one is expected for the Ag^I analogue since the Ag···π and Ag···Ag interactions should be more pronounced.[29a] The $[Ag(tz)]_\infty$ (**12**·Ag) is isostructural to **12**, having an expected

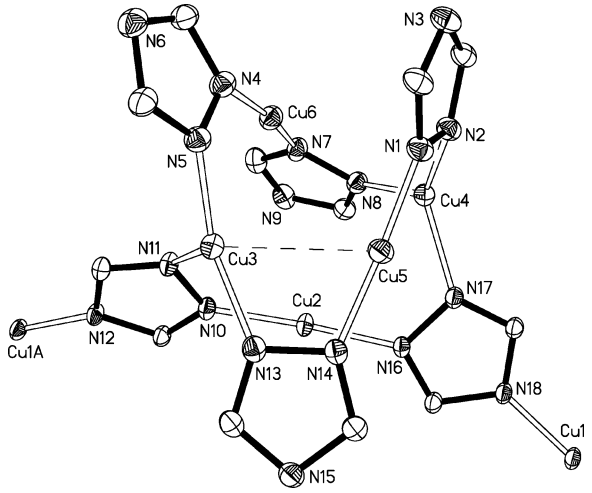

Figure 8. Perspective view of the coordination environments in **5** (thermal ellipsoids: 30%; phenyl groups are omitted for clarity; A: $0.5 - x, -0.5 + y, 0.5 - z$). Selected Cu···Cu separations: Cu3···Cu5 2.899, Cu4···Cu5 3.156, Cu3···Cu6 3.171, Cu4···Cu6 3.223, Cu2···Cu4 3.320, Cu2···Cu3 3.494 Å.

larger crystal cell since the size of silver is significantly larger than that of copper. However, the average plane-to-plane separation is shortened to 3.028 Å, concomitant with shorter intermolecular Ag···Ag separations (3.103, 3.212, 3.430, 3.444 Å) (see Figure S10 in Supporting Information). These observations are in good agreement with our recent discussion on the finite systems.[30]

The topologies of these Cu^I triazolates, in the cases of hydrogen-, methyl-, ethyl- and propyl-substituted ones, can be gradually tuned by the sizes of the substituents. Questions arise for the relation between the structures and the larger substituents such as butyl and phenyl groups. The internal voids of net **C** can be evaluated to have just enough space for the butyl groups. However, long alkyl chains generally occupy more spaces than the calculated value since they cannot be efficiently packed together. Therefore, the proposed **C** net structure for the butyl-substituted ligand is not necessary. Actually, a mixed ligand with cyanide ion (**4**) instead of a binary Cu^I 3,5-dibutyl-1,2,4-triazolate was isolated in our experiments. Presumably, it may be due to the difference in stability of the crystal structures of the proposed **C** net and complex **4**. The C−C bond cleavage and release of cyanide for organonitriles are not surprising under water-containing solvothermal conditions.[13,24] The $M_2(tz)_2$ SBUs should not be the dominant structural units for larger subsituents as there is no possible extended network that can simultaneously satisfy the steric repulsion and free space requirements.

The asymmetric unit of $[Cu_6(phtz)_6]_\infty$ (**5**, Hphtz = 3,5-diphenyl-1,2,4-triazole) contains four linear (Cu−N 1.865(4)−1.876(3) Å, N−Cu−N 169.4(2)−179.5(2)°) and two trigonal (Cu−N 1.908(4)−2.126(3) Å, N−Cu−N 101.4(2)−146.6(2)°) coordinated Cu^I centers, as well as four μ_2- and two μ_3-phtz ligands. The unique structure of **5** can be described as a cluster-based zigzag chain (see Figure S11 in Supporting Information) constructed by Cu^I-linked $[Cu_5(phtz)_6]^-$ cores, in which close Cu···Cu interactions as short as 2.899 Å are found (Figure 8).

In the context of the simplest binary Cu^I triazolates, structural prediction is relatively simple for the alkyl- and phenyl-substituted triazoles, especially for the small ones, since only three possible coordination sites are available. One should never

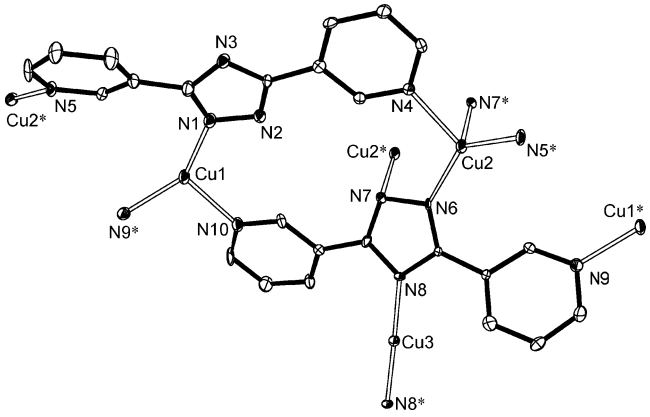

Figure 9. Perspective view of the coordination environments in **7** (thermal ellipsoids: 50%; only one of the two crystallographically independent fragments is shown; hydrogen atoms are omitted for clarity). Selected bond lengths: Cu1−N1 1.958(4), 1.933(3); Cu1−N9 1.977(4), 1.981(4); Cu1−N10 2.099(4), 2.096(4); Cu2−N4 2.134(4), 2.127(4); Cu2−N5 1.988(3), 1.998(3); Cu2−N6 1.972(3), 1.985(4); Cu2−N7 2.358(4), 2.294(4); Cu3−N8 1.857(3), 1.867(3) Å.

Table 3. Emission Data of the Cu^I and Ag^I Complexes

compd	λ_{ex}/nm	λ_{max}/nm	τ/μs	possible origin
1	288	485	11.77(3)	^{3}[MLCT]
2	280	498	1.08(4), 0.222(3)	^{3}[MLCT]
3	275	503	2.123(6)	^{3}[MLCT]
5	330	584	9.27(4)	^{3}[MLCT], ^{3}[MC], ^{3}[MMLCT]
7	366	532	0.400(1)	^{3}[MLCT]
10	356	558	2.83(6), 0.419(6)	^{3}[MLCT] + ^{3}[XLCT]
12	302	468	20.87(8)	^{3}[MLCT], ^{3}[MC], ^{3}[MMLCT]
12·Ag	266	410	$4.69(1) \times 10^3$	$^3[\pi-\pi^*]$
	336	508	$2.58(1) \times 10^{-3}$	^{1}[LMCT]

reasonably predict the coordination number or the extended structure of the 3-pyridyl- and 4-pyridyl-substituted 1,2,4-triazolates since the five nitrogen donors of these ligands are independent, while the coordination number of Cu^I can be as high as four. On the other hand, the local coordination geometries and the possible 0−1D extended superstructure may be readily predicted for the binary Cu^I/Ag^I 2-pyridyl-substituted 1,2,4-triazolate, because the ligand can afford two bidentate chelating sites for accommodation of the Cu^I/Ag^I centers (four-coordinated).[31]

Attempts for the synthesis of a binary Cu^I di(3-pyridyl)-1,2,4-triazolate by our in situ ligand reaction were not successful; a cationic Cu^I di(3-pyridyl)-1,2,4-triazolate network $\{[Cu_5(3\text{-pytz})_4]\cdot NO_3\cdot 2H_2O\}_\infty$ (**7**, 3-Hpytz = 3,5-di(3-pyridyl)-1,2,4-triazole) was isolated in moderate yield instead. The asymmetric unit of **7** contains two types of 3-pytz ligands and three types of Cu^I centers with different coordination modes (Figure 9). A complicated, cationic 2D layer is therefore constructed by the unusual combination of two-, three-, and four-coordinated Cu^I (also observed in **4**), as well as the exo-tridentate and exo-pentadentate 3-pytz ligands (see Figure S12 in Supporting Information).

Photoluminescence Properties. The photoluminescence properties of the coinage d^{10} metal complexes (**1**−**5**, **7**, **10**, **12**, **12**·Ag) have also been studied, and the spectral data are summarized in Table 3. Although we were unable to detect the luminescence of the Cu^I cyanide triazolate **4** at room temperature, all other Cu^I complexes exhibit bright phosphorescence

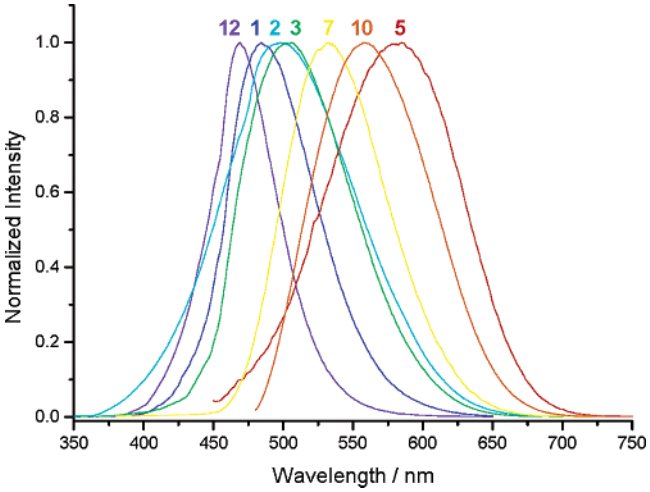

Figure 10. Emission spectra of the Cu^I complexes.

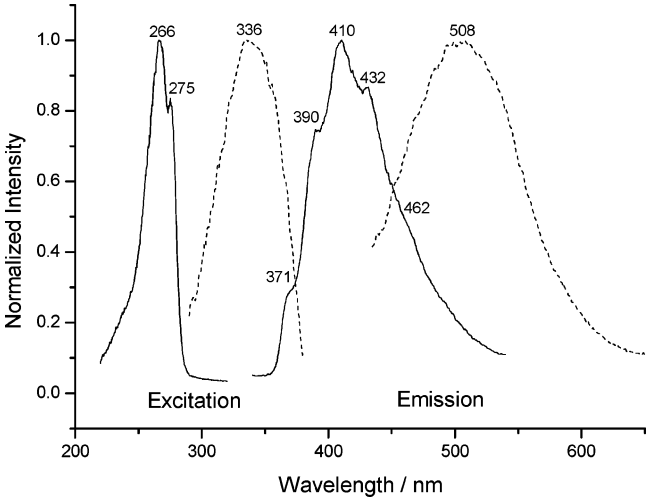

Figure 11. Photoluminescence spectra of **12**·Ag.

at room temperature. We tentatively assigned all of the emissions of the Cu^I complexes to be mainly originated from ^{3}[MLCT] excited states for their broad and structureless emission spectra, as well as their long luminescence lifetimes in the range of microseconds.[42−44] The emission maxima for the Cu^I alkyl-substituted triazolates **1**−**3** are quite similar in the blue to green range, which are in agreement with their relevant ligand structures and dimeric SBUs (Figure 10). The relatively longer lifetime of **1** (11.77(3) μs), compared to those of **2** and **3**, may be ascribed to the different dihedral angles between adjacent planar SBUs. The dense, rigid 2-fold interpenetrating network of **1** should also be responsible the longer lifetime.[43] Moreover, the long alkyl chains are more flexible in **2** and **3**, as indicated by their disordered conformations. Guest molecules may affect the luminescence properties of **2** and **3** since the trigonal-planar-coordinated Cu^I centers in the **C** net structures are open.[45] Compared to those of the virtually dense **3** (2.123(6) μs), the emission peak of the porous **2** is broader and can be divided into two components (1.08(4) and 0.222(3) μs). The emission peak of **12** is slightly blue-shifted, which is in accord with the higher energy of the π*-orbital of the unsubstituted triazolate. Similar to the comparison between **B** and **C** net structures, the longer lifetime of **12** may be related to the **A** net structure. Since the interlayer Cu···Cu contacts are shorter than that inside the $Cu_2(tz)_2$ SBUs, the metal−metal interactions may also affect the emission properties. Therefore, the metal-centered ^{3}[MC] or metal−metal bond to ligand charge transfer ^{3}[MMLCT] excited states should also be possible. This assignment may also be applicable to **5** (9.27(4) μs) featuring shorter Cu···Cu contacts. The large red-shift of the emission maximum of **5** is related to the lower energy of the π*-orbital of the larger π-system of the diphenyl-substituted ligand. For comparison, the lifetime of **7** without short Cu···Cu contact is significantly shorter (0.400(1) μs). Since the lifetime data can be only fitted by a biexponential decay and chloride ions are incorporated in the Cu^I triazolate network, the chloride to ligand charge transfer ^{3}[XLCT] excited states should be involved in the emission of **10**.[42,44]

Interesting photoluminescence phenomena have also been observed for **12**·Ag (Figure 11). A broad emission peak similar to those of the simple Cu^I triazolates (**1**−**3**, **12**) with maximum at 508 nm was observed with 336-nm excitation. We first attributed the emission red-shift compared with the Cu^I analogue to their different coordination abilities and d* orbital energies. However, the lifetime for this emission is only at the nanosecond range (2.58(1) ns, see Figure S13a in Supporting Information), which indicates significant spin-allowed nature. Therefore, we tentatively assigned this emission to the ^{1}[MLCT] excited state. Regarding the oxidative tendency of Ag^I ions, a ^{1}[LMCT] excited state should be more reasonable.[44] Searching for the ^{3}[MLCT] or ^{3}[LMCT] emissions for **12**·Ag at longer wavelengths at room temperature was unsuccessful. On the other hand, an intense emission with vibronic structure was detected at the high energy region (maximum 410 nm). The vibronic progression with a constant spacing of ca. 1250 cm^{-1} is in the range of ν_{C-N} and ν_{N-N} vibrations of several heterocyclic ligands.[46] These observations indicate that this high-energy emission of **12**·Ag is ligand-based. The lifetime data in the millisecond range (4.69(1) ms, see Figure S13b in Supporting Information) suggest that the emission is originated from the 1,2,4-triazolate $^3[\pi-\pi^*]$ excited state.[46−48] The 1,2,4-triazole and the alkyl-substituted ones are not known as strong emitters, and the $^1[\pi-\pi^*]$ emission peaks of these small ligands should lie in the UV region. The $^3[\pi-\pi^*]$ emissions of these ligands may be red-shifted to the visible region; however, they can hardly be detected for the strong spin-forbidden nature of the $T_1 \rightarrow S_0$ processes. The observation of the phosphorescence emission from the 1,2,4-triazolate from **12**·Ag should be ascribed to the internal heavy metal effect, in which the spin-forbidden $T_1 \rightarrow S_0$ processes become allowed by shortening the usually very long lifetimes (seconds for free organic molecules) to milliseconds. Similar examples using internal

(42) Yam, V. W.-W. *Acc. Chem. Rev.* **2002**, *35*, 555−563.
(43) (a) Zheng, S.-L.; Yang, J.-H.; Yu, X.-L.; Chen, X.-M.; Wong, W.-T. *Inorg. Chem.* **2004**, *43*, 830−838. (b) Zheng, S.-L.; Chen, X.-M. *Aust. J. Chem.* **2004**, *57*, 703−712.
(44) Ford, P. C.; Cariati, E.; Bourassa, J. *Chem. Rev.* **1999**, *99*, 3625−3647.
(45) Lu, W.; Chan, M. C. W.; Zhu, N.-Y.; Che, C.-M.; He, Z.; Wong, K.-Y. *Chem.−Eur. J.* **2003**, *9*, 6155−6166.
(46) Omary, M. A.; Rawashdeh-Omary, M. A.; Diyabalanage, H. V. K.; Rasika Dias, H. V. *Inorg. Chem.* **2003**, *42*, 8612−8614.
(47) (a) Che, C.-M.; Chao, H.-Y.; Miskowski, V. M.; Li, Y.-Q.; Cheung K.-K. *J. Am. Chem. Soc.* **2001**, *123*, 4985−4991. (b) Chao, H.-Y.; Lu, W.; Li, Y.-Q.; Chan, M. C. W.; Che, C.-M.; Cheung, K.-K.; Zhu, N.-Y. *J. Am. Chem. Soc.* **2002**, *124*, 14696−14706.
(48) Wong, W.-Y.; Liu, L.; Shi, J.-X. *Angew. Chem., Int. Ed.* **2003**, *42*, 4064−4068.

heavy metal effects via d^{10} metal coordination have been used to enhance the phosphorescence of organic molecules recently.[46−48] No ligand based $^3[\pi-\pi^*]$ emission was detected for the Cu^I complexes at room temperature, in which the weaker heavy metal effect of the copper ion should be partially responsible.

Conclusions

The unusual one-pot syntheses of the 3,5-disubstituted-1,2,4-triazole have been extended for alkyl-, phenyl-, and pyridyl-substituted nitriles. By using controlled solvothermal methods, we have trapped the intermediate 1,3,5-triazapentadiene in its deprotonated form in a neutral Cu^{II} complex **8**, which can also be synthesized via Ni^{II}-assisted coupling of nitrile and ammonia. However, only Cu^{II} rather than Ni^{II} can promote the ring closure procedure for the final 1,2,4-triazole. Being different from the traditional hydrazine-based syntheses of 1,2,4-triazole, organonitrile, ammonia, and Cu^{II} ion are necessary for this unique reaction, and the N−N bond is formed in the final step. Other ligand reactions such as hydrolysis and C−C bond cleavage were also found, which emphasize the negative effects of water, although our triazole synthesis can also be performed in the aqueous environment.

On the basis of two novel coordination networks of the binary Cu^I methyl- and propyl-substituted triazolates previously reported, we were able to find the difference and relationship of the simple but important 3- or 4-connected topologies,[12] leading to the rational construction of the close-packed 2D networks of two binary Cu^I/Ag^I nonsubstituted triazolates, as well as one 3D porous structure of the Cu^I ethyl-substituted triazolate. The synthesis of the isostructural Ag^I coordination polymer indicates that the network prototypes present in the Cu^I compounds can be further modified by changing the metal centers. As expected, the ligands with substitutents larger than the propyl group feature other structures instead of the related 3- or 4-connected networks. In contrast, prediction of the crystal structures for more complicated ligand containing additional nitrogen donors was inaccessible. Therefore, we may consider the present work as giving a close insight into the crystal engineering in the context of ligand design and structure prediction.

The photoluminescence analysis of the Cu^I complexes has been simplified since the alkyl-substibituted and nonsubstituted 1,2,4-triazoles are very small π-conjugated systems. The emission spectra and lifetime data are both in good agreement with our assignments of the triplet excited state of these Cu^I triazolate networks. On the other hand, the Ag^I triazolate exhibits interesting photoluminescence phenomena, including the long-life triplet organic emission. The redox and heavy-atom effect differences between Ag^I and Cu^I and the relatively high-lying π^*-orbital of the simple 1,2,4-triazolates are responsible for these observations.

Acknowledgment. This work was supported by the National Natural Science Foundation of China (Grant No. 20131020), Ministry of Education of China (Grant No. 01134 and Grant No. 20020558024), and Guangdong Provincial Science and Technology Bureau.

Supporting Information Available: Crystallographic data in CIF format, additional plots, and photoluminescence data for the complexes in PDF format. This material is available free of charge via the Internet at http://pubs.acs.org.

JA042222T